

Shaking earth: Non-linear seismic processes and the second law of thermodynamics: A case study from Canterbury (New Zealand) earthquakes

A. Posadas^{a,b,*}, J. Morales^{a,c}, J.M. Ibañez^{a,c}, A. Posadas-Garzon^d

^a Instituto Andaluz de Geofísica, Campus Universitario de Cartuja, Universidad de Granada, 18071 Granada, Spain

^b Departamento de Química y Física, Universidad de Almería, 04120 Almería, Spain

^c Departamento de Física Teórica y del Cosmos, Universidad de Granada, 18071 Granada, Spain

^d Facultad de Ciencias, Universidad de Granada, 18071 Granada, Spain

ARTICLE INFO

Article history:

Received 30 April 2021

Revised 23 June 2021

Accepted 25 June 2021

Available online 16 July 2021

Keywords:

Nonlinear dynamics

Earthquakes

Second law of thermodynamics

Entropy

Canterbury earthquakes

ABSTRACT

Earthquakes are non-linear phenomena that are often treated as a chaotic natural processes. We propose the use of the Second Law of Thermodynamics and entropy, H , as an indicator of the equilibrium state of a seismically active region (a seismic system). In this sense, in this paper we demonstrate the exportability of first principles (e.g., thermodynamics laws) to others scientific fields (e.g., seismology). We suggest that the relationship between increasing H and the occurrence of large earthquakes reflects the irreversible transition of a system. From this point of view, a seismic system evolves from an unstable initial state (due to external stresses) to a state of reduced stress after an earthquake. This is an irreversible transition that entails an increase in entropy. In other words, a seismic system is in a metastable situation that can be characterised by the Second Law of Thermodynamics. We investigated two seismic episodes in the Canterbury area of New Zealand: the 2010 Christchurch earthquake ($M = 7.2$) and the 2016 Kaikoura earthquake ($M = 7.8$). The results are remarkably in line with our theoretical forecasts. In other words, an earthquake, understood as an irreversible transition, must results in an increase in entropy.

© 2021 The Author(s). Published by Elsevier Ltd.

This is an open access article under the CC BY-NC-ND license (<http://creativecommons.org/licenses/by-nc-nd/4.0/>)

1. Introduction

One of the great challenges of modern seismology is characterising the chaotic and non-linear behaviour of earthquakes, of any size and in any environment, tectonic or volcanic. This handicap is reinforced by the physical impossibility of accessing direct observations (or measurements) owing to the short observation period, which makes it difficult to record multiple ruptures of the same location or fault segment. Such behaviour suggests that earthquakes are not stochastic. Together, these issues are why earthquakes remain unpredictable physical phenomena. However, earthquakes are precise physical phenomena associated with the exchange of energy, during both accumulation and deformation processes, and during processes of rupture and propagation in the form of seismic waves. As such, earthquakes represent a physical system that

is moving from equilibrium to non-equilibrium, where an increase and decrease in the internal energy of the system is observed continuously, and stochastic processes cannot be used to define it. On this basis, the laws of thermodynamics, and fundamentally the Second Law, or the use of entropy, is a useful tool to describe this phenomenon.

The Zero, First, and Second laws (or principles) of Thermodynamics lead to the definition of three state functions. From the Zero Law, temperature (T) as a state function is deduced. From the First Law, internal energy (U) as a state function is deduced. Finally, from the Second Law, entropy (S) is deduced. On one hand, temperature is associated with the state of thermal equilibrium, and internal energy establishes the conversion between heat and work. In addition, entropy can be calculated as the maximum of the Boltzmann function, $-H(t)$, over all possible states that a system can access or as the time limit of that function [1,2]. For this reason in many fields of science, it is possible to use $-H(t)$ as an indicator of the evolution of a certain system; for instance, entropy is used in cosmology [3], climatology [4,5], life sciences [6,7],

* Corresponding author.

E-mail address: aposadas@ual.es (A. Posadas).

chemistry [8], languages [9], and social sciences [10]. In seismology, entropy can be used to identify future states in a region of Earth's crust based on its current state [11,12]. A detailed review of the entropy concept is provided in Appendix A.

The Second Law can be applied to the study of earthquakes in order to better understand their spatio-temporal distribution and magnitudes. In particular, the application of this Law to the study of the distribution of magnitudes is crucial. Magnitude reflects the release of accumulated elastic energy, and so is evidence of the generation of irreversible processes.

Spatial and temporal patterns of seismicity should vary as a result of the stress field applied to a volume of the Earth's crust. Modelling of the distribution of earthquakes reflects a physical system characterised by chaotic processes [13]. This system, called the 'seismic system' by some authors [14], continuously suffers reorganization of stresses from an equilibrium state to a non-equilibrium state with the occurrence of each earthquake. De Santis et al. [15] states that, in seismology, the occurrence of an earthquake can be considered as a phase transition (the authors also review and clearly explain, the importance of using entropy to understand seismic phenomenon holistically). Therefore, seismic activity is viewed as a non-equilibrium statistical process [16] where the energy released by earthquakes is not transformed integrally into tectonic energy. From the perspective of the Second Law, this reorganization is reflected in the values of entropy; the postulates that only those phenomena for which entropy (see Appendix A) increases in the whole Universe are allowed. Thus, in the field of seismology, the Second Law can be used to ascertain future states of a region of the Earth's crust from its current state [11]. A brief review of the use of entropy in seismology is given in Appendix B.

In this study, we established a methodology based on changes in the value of entropy, as identified by De Santis et al. [17], when an earthquake occurs. The proposed technique is novel from two points of view. Firstly, we systematically established the theoretical steps necessary to determine entropy—(1) calculate the threshold magnitude M_0 , (2) evaluate the windowing process and the width of the window (W) and, (3) compute H . In addition, error is considered in the results. Secondly, the chosen application is not applied to a seismic system with a single event. Instead, we show that when two earthquakes occur in the same seismic system, the value of H recovers after the first seismic episode and grows again after the second, returning to the original values when stresses return to equilibrium.

With respect to a systematic methodology for determining H , we identified the relationship between the value of parameter b from the Gutenberg-Richter relationship and the value of the entropy, H . Secondly, error calculation in b was established, allowing error in H to be quantified through a new formula (Eq. 18). Thirdly, we detail the common methods for determining the threshold magnitude M_0 ; the use of the Maximum Curvature (MAXC) technique is expressly proposed [18].

To test our methodology, we applied it to two seismic episodes in the Canterbury area of New Zealand: the 2010 Christchurch earthquake ($M = 7.2$) and the 2016 Kaikoura earthquake ($M = 7.8$). These events were chosen both for their global tectonic interest, and for the fact that while initially considered as classic mainshocks-aftershocks seismic sequences, when individually reviewed and placed in their tectonic context, they were found to represent temporal and energetic anomalies.

2. Methods and data

2.1. Second law of thermodynamics and magnitude distribution

The distribution of earthquake magnitudes follows an empirical and universal relationship, usually called the Gutenberg-Richter re-

lationship (GRr) [19]:

$$\log n(M >) = a - bM \tag{1}$$

where $n(M >)$ is the cumulative number of earthquakes with magnitude equal to or larger than M , and a and b are real constants that may vary in space and time. Parameter a characterises the general level of seismicity in a given area during the study period (i.e., the higher the a value, the higher the seismicity), whereas parameter b , which is typically close to 1, describes the relative abundance of large to smaller shocks.

Many works have tried to identify the physical meanings of these parameters; for example, Jimenez et al. [20] studied long-run correlations in a seismic catalogue (the Iberian Peninsula catalogue recorded from 1970 to 2001) by means of the Hurst exponent and proved that seismicity rate (a value) provides the best measure of the predictability in an earthquake system. However, it is the b parameter that has been the main focus of interest, perhaps owing to the almost universality of its value (i.e., close to unity everywhere in the world). Most studies have found the range of b to be 0.6–1.2 (e.g., Frohlich and Davis [21], Wesnousky [22], and, recently, Singh et al. [23]); however, we can expect larger b values (> 1.3) for some open systems such as volcanoes (e.g., Turcotte [24] and Wiemer and McNutt [25]).

It is accepted that the b value depends on the stress regime and tectonic character of the region [26,27]; a recent study found that the b value of the GRr is an indicator of rock failure processes [28]. Others interpretations of b can be found in, for instance, Wiemer and Benoit [29] and Wiemer et al. [30], who identified volumes of active magma bodies, Turcotte [24] who confirmed the relationship between fractal dimension D and b ($D = 2b$), Gibowicz and Lasocki [31] who related b with induced seismicity, Monterroso and Kulhanek [32] who studied the roots of regional volcanism, and Monterroso [33] and Nuannin et al. [34] who used values of b to forecast major tectonic earthquakes. However, the most interesting relationship is between the a and b values and the Second Law (i.e., entropy).

Berrill and Davis [35], Shen and Manshina [36], Main and Burton [37], and Feng and Luo [38] all consider $p(M)$ to be the probability density function of magnitude for earthquakes and, following Eq. A9, the Shannon information entropy is:

$$H(p) = - \int_{M_0}^{\infty} p(M) \cdot \log p(M) \cdot dM \tag{2}$$

where M_0 is the threshold magnitude. There are two restrictive conditions. First:

$$\int_{M_0}^{\infty} p(M) dM = 1 \tag{3}$$

The other restrictive condition arises from the fact that the average value of all possible magnitudes \bar{M} , in certain period of time, is:

$$\bar{M} = \int_{M_0}^{\infty} M p(M) dM \tag{4}$$

The Second Law requires that there exists a distribution under which H would be at its maximum value but under two restrictive conditions; that is, the spontaneous development of the system from a state of non-equilibrium to a state of equilibrium is a process in which entropy increases and the final state of equilibrium corresponds to the maximum entropy. Then, the problem can be solved by applying the Lagrange multiplier method; to do that, we define the lagrangian \mathcal{L} as:

$$\mathcal{L} (p(M)) = H(p(M)) - \lambda_1 \int_{M_0}^{\infty} p(M) dM - \lambda_2 \int_{M_0}^{\infty} M p(M) dM \tag{5}$$

where λ_1 and λ_2 are Lagrange's multipliers; then, it is possible to deduce the probability density function in the form [38]:

$$p(M) = \frac{1}{\bar{M} - M_0} \exp\left(-\frac{M - M_0}{\bar{M} - M_0}\right) \quad (6)$$

If we have N earthquakes:

$$p(M) = \frac{n}{N} \quad (7)$$

then, we match both formulas and take logarithms to get:

$$\log n = \log\left(\frac{N}{\bar{M} - M_0}\right) + \frac{M_0 \cdot \log(e)}{\bar{M} - M_0} - \frac{\log(e)}{\bar{M} - M_0} \cdot M \quad (8)$$

from which the identifying terms from GRr are:

$$a = \log\left(\frac{N}{\bar{M} - M_0}\right) + \frac{M_0 \cdot \log(e)}{\bar{M} - M_0} \quad (9)$$

and

$$b = \frac{\log(e)}{\bar{M} - M_0} \quad (10)$$

Hence, the probability density function (Eq. 6) can be rewritten as:

$$p(M) = \frac{b}{\log(e)} \cdot 10^{-b(M - M_0)} \quad (11)$$

Substituting into Eq. 3, we get [15]:

$$H = - \int_{M_0}^{\infty} \frac{b \cdot 10^{-b(M - M_0)}}{\log(e)} \cdot \log\left(\frac{b \cdot 10^{-b(M - M_0)}}{\log(e)}\right) dM = - \log(b) + \log(e \cdot \log(e)) \quad (12)$$

This result is general and does not depend on the seismic sequence to be studied; secondly, it is obtained from the Second Law and allows us to interpret the meaning of the b parameter in terms of entropy. De Santis et al. [17] stated that is not a simple rescaling of b and declared that the main contribution of their work, with respect to previous studies on GRr analysis, is Eq. 10. They applied this formula to an Abruzzi region seismic sequence (that of the L'Aquila 2009 earthquake) and to the Colfiorito, Umbria-Marche sequence (1997). The last equation only can be used if $b \leq \log(e \times \log e) \approx 1.18$ in order to have $H \geq 0$ [17].

On the other hand, Aki [39] and Utsu [40] were the first to describe the Maximum Likelihood Estimation method to obtain the b value; they considered the magnitude M to be a continuous random variable and showed that if GRr holds, then the probability density function is:

$$p_{Aki-Utsu}(M) = \frac{b}{\log(e)} \cdot \frac{10^{-bM}}{10^{-bM_{min}} - 10^{-bM_{max}}} \quad (13)$$

where M_{min} and M_{max} are the minimum and maximum magnitude in the catalogue, respectively. When $M_{max} \gg M_{min}$ in Eq. 13 becomes Eq. 11; for instance, Marzocchi and Sandri [42] suggest that $M_{max} - M_0 \geq 3.0$ [41]; alternatively, Lolli and Gasperini [42] point out that it is sufficient for $M_{max} - M_0 \geq 2.0$, whereas De Santis et al. [17] indicated that is valid when M_{min} is significantly lower than the largest expected magnitude. Furthermore, Eq. 10 is also obtained by using the Aki [39] and Utsu [40] statistical formulas; Utsu [43] suggested a slight modification of Eq. 10 after considering that the lowest binned magnitude (i.e., the threshold magnitude) contains all the magnitudes in the range:

$$M_0 - \Delta M/2 \leq M < M_0 + \Delta M/2 \quad (14)$$

where ΔM is the resolution of the magnitude (usually $\Delta M = 0.1$), and thus the real minimum magnitude is [44]:

$$M_{min} = M_0 - \Delta M/2 \quad (15)$$

Consequently, after the Utsu [43] correction, Eq. 10 becomes:

$$b = \frac{\log(e)}{\bar{M} - (M_0 - \frac{\Delta M}{2})} \quad (16)$$

Finally, the Aki [39] and Utsu [40,43] formulas show that the uncertainty associated with the b value, interpreted as the error in the b value determination, is given by:

$$\sigma_b = \frac{b}{\sqrt{N}} \quad (17)$$

where N is the number of earthquakes considered to compute b. Other estimations of b uncertainty were made by Shi and Bolt [45] and Amorèse et al. [46]; however, in applied methods such as that proposed here, the formulas of Aki [39] or Utsu [40,43] are sufficient [17].

In summary, our proposed approach includes three analysis steps:

- 1 First, the value of M_0 is a critical choice. There are two main classes of methods to evaluate M_0 [47]: catalogue-based methods (e.g., Rydelek and Sacks [48], Woessner and Wiemer [49], and Amorèse [50]) and network-based methods (e.g., Kvaerna and Ringdal [51], Schorlemmer and Woessner [52], D'Alessandro et al. [53]). We used a catalogue-based method because the necessary inputs were available from our dataset. Although some studies estimate the value of M_0 by fitting GRr to the observed frequency-magnitude distribution (the magnitude at which the lower end of the frequency-magnitude distribution departs from the GRr is taken as an estimate of M_0) [54], there are several other methods that can help us to a better determine the threshold magnitude. Some of the catalogue-based techniques include the day-to-night noise modulation (day/night method) [48], the M_0 from the Entire Magnitude Range [55], the MAXC technique [18], the Goodness-of-Fit Test (GFT) [18], the M_0 by b-value stability (MBS) approach [56], and the Median-based analysis of the segment slope (MBASS) [50]. The maximum curvature technique is mainly used in applied techniques and was chosen here; however, the results do not differ significantly among these approaches.
- 2 Second, the time interval W is determined for the calculation of entropy. In other words, the minimum number of earthquakes is used to calculate H. Moreover, the time interval can be chosen using a cumulative, moving, or overlapping earthquake window. On the whole, the final window size will be a reasonable compromise between required resolution and smoothing results. The width of the window can be chosen following the criteria of De Santis et al. [17] based on meaningful values of b; in short, considering that 200 events are the minimum number of events to perform a robust statistical estimation of the quantities b and H. This is also confirmed by previous statistical analyses of a and b values [57]. However, larger values of W could be adopted depending on the relative error made when entropy is computed. Here, the results are presented with a cumulative window, which presents greater stability when only one event is studied, or with a moving window when we want to avoid the memory effect. Nevertheless, the results are substantially the same regardless of the approach taken.
- 3 Finally, the entropy function is obtained for each time t following Eq. 12. By convention, the time attributed to each point of the analyses is the time of the last seismic event considered in each window. The occurrence of a large earthquake (or the accumulation of several important ones) is expected to lead the seismic system to a state of greater disorder; that is, the earthquake is an irreversible transition to a new state, which means an increase in entropy. Once the mainshock is over, entropy returns to stable values.

2.2. Seismological setting and dataset

New Zealand is located on the margin between the Australian and Pacific tectonic plates, where an oblique relative convergent scenario accommodates around 30–50 mm/yr [58,59]. Since 1850, 20 earthquakes with magnitudes larger than 7.0 have occurred in New Zealand. The largest, the 1855 Wairarapa earthquake, occurred near the capital city of Wellington; its magnitude is estimated to have reached 8.2 [60]. The high seismicity reflects a complex tectonic structure where plate boundary deformation creates a south-easterly advancing repetitive structural pattern governed by the propagation of northeast-striking thrust assemblages [61]. As a result, New Zealand experiences many types of faults and earthquake sources: besides subduction zone earthquakes in the Hikurangi and Puysegur trenches, there are shallow strike-slip and thrust earthquakes, normal faulting earthquakes in the back arc of the North Island, and volcanic earthquakes [62].

With respect to the northern South Island, on the one hand, the Pacific tectonic plate (in the east) is subducting beneath the Australian plate (in the west); however, the southern South Island sits on the Australian plate, which is subducting beneath the Pacific plate [63]. Canterbury is located in the central-eastern South Island and Christchurch is the South Island's largest city (and the country's second-largest urban area). The present study deals with two large events that occurred in the Canterbury region—the 2010 M 7.2 Christchurch earthquake and the 2016 M 7.8 Kaikoura earthquake—consequently, seismic activity analysis was constrained to the period between 1 January 2000 and 31 December 2020 in the area defined by 171E–175E and 41S–45S. The seismic catalogue was obtained from GeoNet, a collaboration between GNS Science and the Earthquake Commission of New Zealand.

The first seismic crisis (Fig. 1) extended from late 2010 through to January 2012. On 4 September 2010, the M 7.2 earthquake struck 30 km west of Christchurch; fortunately, there were no associated deaths. It was followed by an aftershock sequence that included around 3000 aftershocks of magnitude greater than 3 [64]. Two larger aftershocks, M 6.2 on 22 February and M 6.0 on 13 June 2011, heavily damaged Christchurch city; 185 people died, 2000 were injured, and ~105 buildings were affected. A third aftershock of M 5.9 took place on 23 December 2011 (Fig. 2) [65].

The second seismic crisis (Fig. 1 and Fig. 2) was located along the north-east coast of the South Island, in the northern Canterbury region near the border with Marlborough. On 13 November 2016, a large magnitude (M = 7.8) earthquake struck; the epicentre was located 60 km southwest of Kaikoura [65]. This earthquake is considered one of the most complex ruptures ever [66]; the complexity was highly unusual and was due to multiple rupturing processes along a large number of unconnected (widely spatially separated) fault segments, all of which broke at the same time.

3. Results

The seismic catalogue includes 35,267 earthquakes in the Canterbury region. In magnitude versus time and monthly seismic graphs (Fig. 2), large magnitude events and the seismic sequences of 2010 and 2016 are clearly visible. In both cases, more 3,000 earthquakes occurred in the months following the main shocks. To detect the entropy changes after the 2010 earthquake, we analysed the catalogue from 2000 to 2015 (catalogue NZ1, which contains 21,094 earthquakes). Next, the rest of the catalogue (i.e., until 2020) was added (catalogue NZ2, which contains 35,267 earthquakes) and used to identify entropy change indicating the occurrence of subsequent earthquakes.

First, the threshold magnitude was needed. Fig. 3 shows the GRr for NZ1; using the MAXC technique [18], we choose a threshold of $M_0 = 2.5$. The final dataset included 13,785 earthquakes.

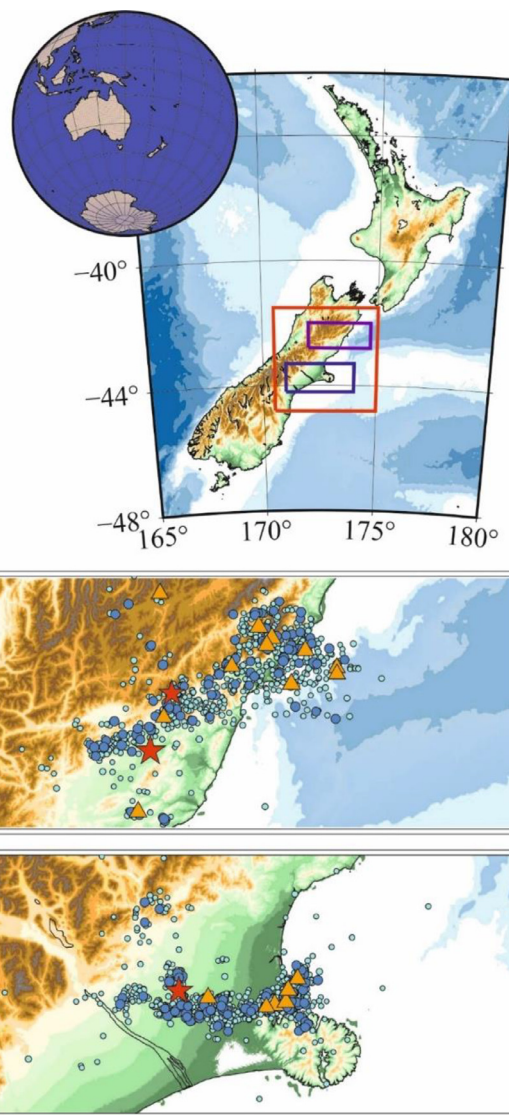


Fig. 1. Study area maps. Canterbury region (red rectangle) of New Zealand, within which purple and blue boxes indicates the Kaikoura and Christchurch epicentral areas, respectively. Epicentres for earthquakes with magnitude of > 3.5 (cyan circles), > 4.5 (blue circles), > 5.5 (orange triangles), and > 6.5 (red stars) for Kaikoura area (up) and Christchurch area (bottom).

The next step is to determine the windowing mode (cumulative, sliding, or partial overlapping) and value of the width of the window (W). As discussed, the results are similar regardless of the windowing process; therefore, in the case of NZ1 we chose the most stable approach (cumulative windowing). The choice of the window width W must consider that values of b should be significant, and so a minimum value of $W = 200$ earthquakes was established. One way to objectify this choice of W is to study the relative error made in obtaining the entropy. From Eqs. 13 and 18, for an entropy value of H , the error margins are:

$$\Delta H = \log \left(\frac{b + \Delta b}{b - \Delta b} \right) \tag{18}$$

Hence, the relative error can be calculated as:

$$\varepsilon (\%) = \frac{100}{H} \cdot \log \left(\frac{b + \Delta b}{b - \Delta b} \right) \tag{19}$$

Fig. 4 shows the relative error as a function of the given initial window width. The cyan line, for instance, corresponds to an ini-

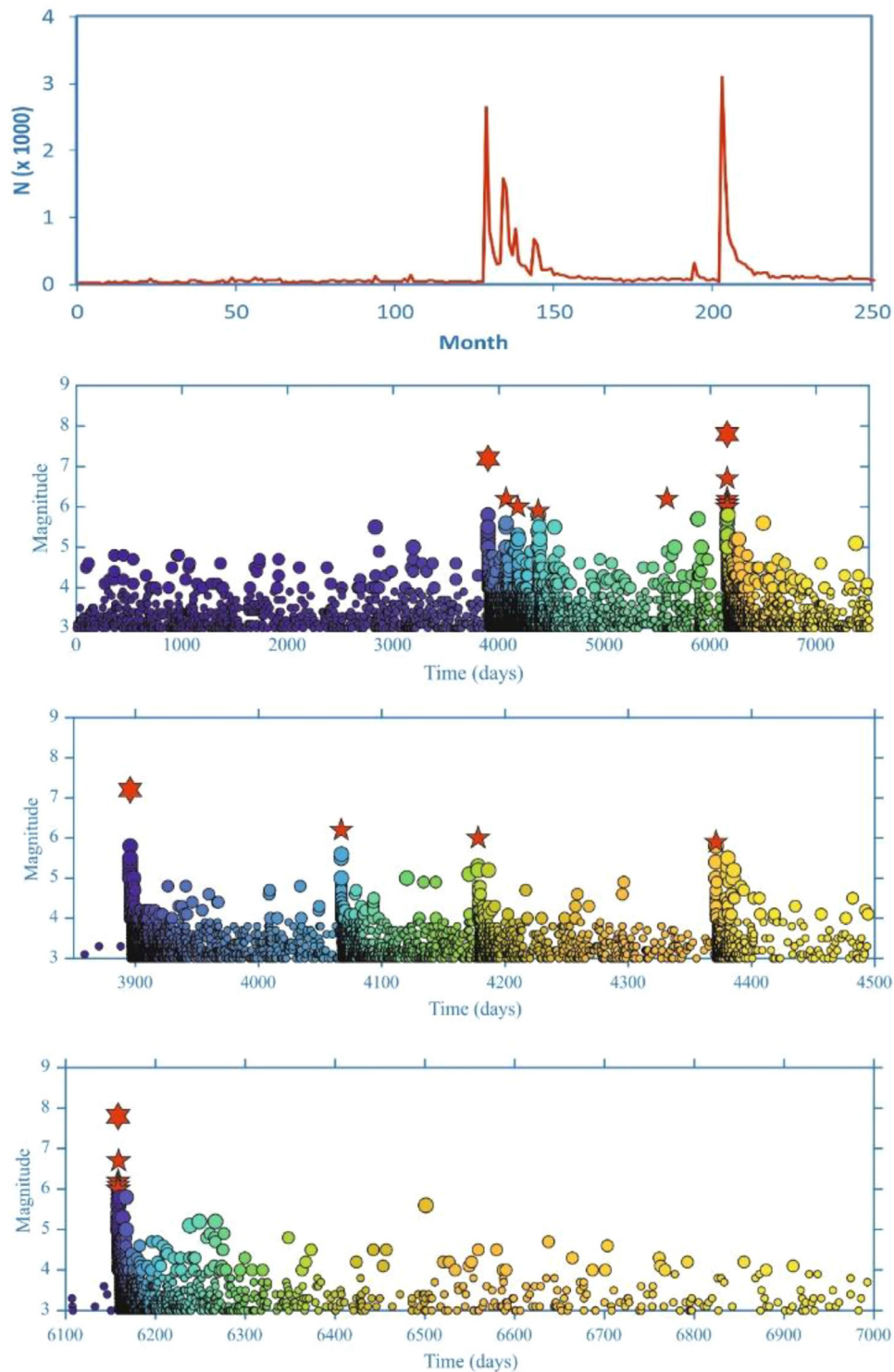


Fig. 2. Seismic activity in the Canterbury region. First plot corresponds to Monthly activity from 2000 to 2020. Peaks are clearly visible in month number 129 (September 2010, relating to the Christchurch seismic sequence) and month number 203 (November 2016, relating to the Kaikoura seismic sequence). After the first main shock in Christchurch ($M = 7.2$), more than 14,000 events occurred in the area over 2.5 years (35 of them of $> M = 5.0$); after the second main shock in Kaikoura ($M = 7.8$), more than 10,000 earthquakes occurred within 2 years (42 of them of $> M = 5.0$). Second graph shows Magnitude versus time (in days) from 2000 to 2020. Third and fourth graphs show Magnitude versus time (in days) for Christchurch seismic sequence (note the three aftershocks with magnitudes $M = 6.2$, $M = 6.0$, and $M = 5.9$ marked with red stars) and for the Kaikoura seismic sequence (five aftershocks with magnitudes $M = 6.7$, $M = 6.2$, $M = 6.1$ and with $M = 6.0$ are marked with red stars).

tial window width of $W = 100$, for which calculated relative error in entropy is 5.4%. As the window width increases, the error decreases; thus, when the window width is 1200 earthquakes (200 initials plus 1000 cumulatively added), the error is barely 2%. Similarly, for a window of $W = 1000$ earthquakes (yellow line), the

relative error of entropy is close to 2%; when the window becomes 2000 earthquakes (1000 initial and 1000 accumulated), the relative error is equal to 1%. Overall, the relative errors of entropy range between 0.5% and 2% for window widths with > 1000 cumulative earthquakes. In any case, as stated above, the choice of W must be

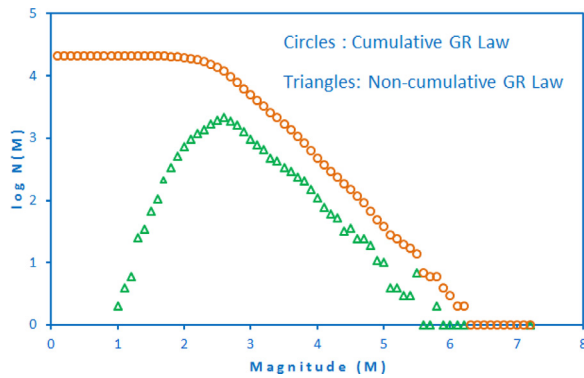


Fig. 3. Gutenberg-Richter (GR) law for the Christchurch seismic sequence. Orange circles indicate the cumulative number of earthquakes; green triangles denote the non-cumulative number of earthquakes. Based on the Maximum Curvature (MAXC) technique [18], we selected a magnitude threshold of $M_0 = 2.5$.

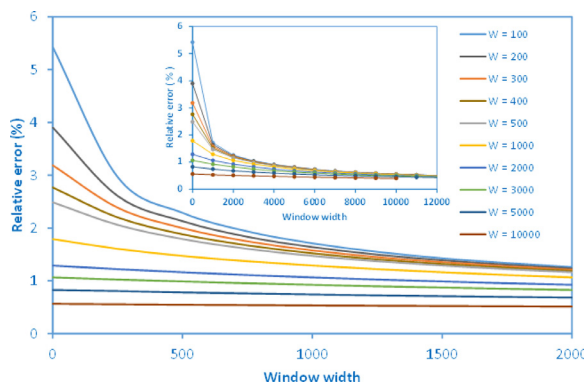


Fig. 4. Relative error ε for the Christchurch earthquakes (calculated using Eq. 18). The insert graph shows ε for a given initial window width (from $W = 100$, cyan line, to $W = 10000$, brown line) and it ranges to 12,000 earthquakes (the whole series). The main graph shows a window width zoom from 0 until 2000 events. The ε ranges between 0.5% and 2% for window widths of > 1000 cumulative earthquakes.

a reasonable compromise between calculated errors and the visibility of the results.

Based on $W = 200$ earthquakes (i.e., the minimum reasonable value), the entropy, as a function of time, can be seen in Fig. 5. We found that 2000 days before the Christchurch earthquake, the entropy values were approximately constant; however, with the main shock ($M = 7.2$, on 3 September 2010), the value of H doubled, indicating that an irreversible phase transition had taken place. In the days immediately after the main event, the entropy decreased; we interpret this as a new equilibrium state characterised by new stress and strain fields. Following a subsequent $M = 6.2$ event on 21 February, the entropy again increased. This sequence was repeated twice more with earthquakes of $M = 6.0$ (13 June 2011) and $M = 5.9$ (23 December 2011). Finally, 2000 days after the main shock, entropy was continuing to decrease, indicating that the system was evolving towards a stable situation.

This analysis corresponds to a cumulative window process; Fig. 6 shows the same analysis but using a moving window process ($W = 1500$, for which relative error is $< 1\%$). The results are qualitatively identical.

Finally, we tested whether our hypothesis would hold when the chosen seismic system was expanded; in other words, when the Kaikoura 2016 seismic sequence was also considered. For this joint study, the data file previously described as NZ2 was used. The GRr for NZ2 is shown in Fig. 7. Based on the MAXC technique, we established a threshold of $M_0 = 2.25$, yielding a dataset of 26,163 earthquakes.

By using the moving windowing process ($W = 1500$ earthquakes), we avoided the memory effect of past earthquakes; the results are shown in Fig. 8. We found that H exhibited the same behaviour as that described for the Christchurch sequence; however, we can now see that its initial values (after the Christchurch sequence) had recovered prior to the 2016 Kaikoura earthquake.

4. Discussion

Our study shows that it is possible to associate changes in entropy, H , with the occurrence of significant seismic events in a given area. The relationship between H and the value of the parameter b in the well-known Gutenberg-Richter law was introduced by Feng and Luo [38] among others; De Santis et al. [17] provided two tests based on Italian seismic sequences of moderate magnitude earthquakes, including the 2009 $M 6.3$ L'Aquila 2009 and 1997 $M 6.0$ Colfiorito 1997 events. In the present paper, the robustness of this technique is confirmed; moreover, we have expanded the approach to allow it to be extended to various events in the same area. From a thermodynamic point of view, an increase in H is associated with an irreversible transition from one state to another. This has been confirmed both on a small scale [27] and a large scale [e.g., Parsons et al. [67]. Even for quiescent seismic sequences, where is a relative decrease in the number of earthquakes or energy within a certain time interval in comparison with long-term observations in the same region, H could decrease and could be used as a precursor parameter (e.g., Hainzl et al. [68], Rudolf-Navarro et al. [69]).

Our results show that entropy is a geophysical observable that can improve understanding of elastic energy accumulation inside the Earth. To date, most of the regions studied from this perspective are so-called tectonic regions (i.e., regions in which large earthquakes occur). However, other regions, and in particular volcanic regions, are also dominated by energy accumulation processes, including non-linear and quasi-static processes. Volcanic seismicity does not follow the Gutenberg-Richter law (e.g., Ibáñez et al. [70]) or the propagation of stresses and deformation is not a linear process (e.g., Díaz-Moreno et al. [71]). For this reason, in addition to new insight into the seismic series analysed, we believe that this study opens an important door for application of this approach to other processes of the Earth's interior dynamics.

The choice of New Zealand earthquakes was not arbitrary; in large part, this case study was chosen owing to the high quality of the data provided by GeoNet. However, it was also chosen because it provided data on the occurrence of two large earthquakes in the same region (albeit on different fault systems) within a short timespan (6 years). Even considering the two separate fault systems, it is unusual for two large earthquakes to occur so close together (epicentral distances < 300 km) and so close in time. Recurrence periods in New Zealand are considerable (e.g., Langridge et al. [72]), and can be estimated from probabilities based on continuous monitoring and from our knowledge of fault rupture histories. Recurrence periods in the study area range from 500 years (Wellington Fault for a $M = 7.0$ earthquake) to 1200 years (Wairarapa Fault for a $M = 8.0$ earthquake); nonetheless, the Kaikoura earthquake occurred only 6 years after Christchurch event. Such events demonstrate the need for tools and methodologies to facilitate seismic prediction studies.

Moreover, the Christchurch earthquakes revealed the complexity of the crust in the region. For instance, the main shock in September and the $M = 6.2$ aftershock in February occurred on previously unknown faults [64]; this most likely reflects the fact these earthquakes take place in an immature intra-plate setting, with little seismic activity prior to this sequence [73]. Moreover, some factors (tectonic, seismic, source spectra, and stress drop) suggest that that the second earthquake was not an aftershock, but

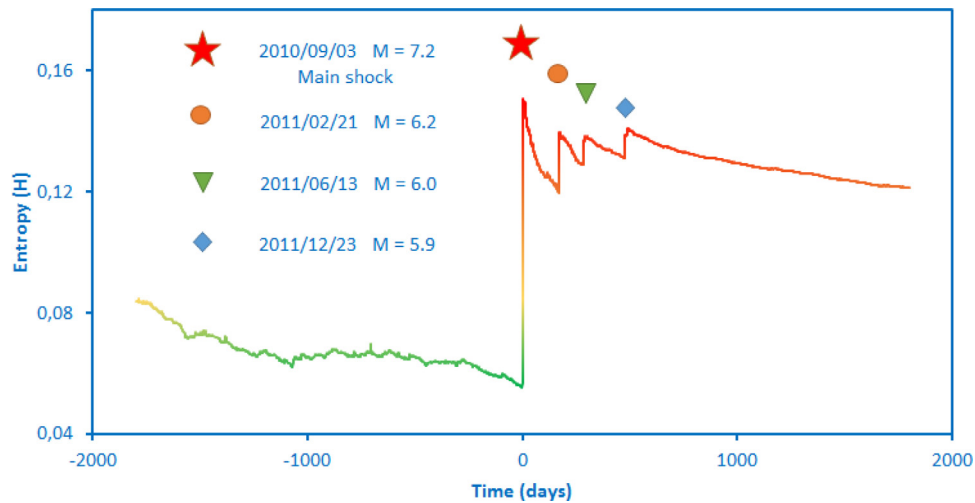


Fig. 5. Entropy, H , versus time (in days with respect to the date of the main event; that is, 4 September 2010) during the Christchurch sequence. The windowing process was carried out with a cumulative window width starting at $W = 200$ earthquakes. The H saw an abrupt increase on the day of the main event (red star) and a decrease after it. It increased again with the first aftershock ($M = 6.2$, orange circle) and then decreased. This pattern was repeated for two further aftershocks ($M = 6.0$, green triangle; $M = 5.9$, blue diamond).

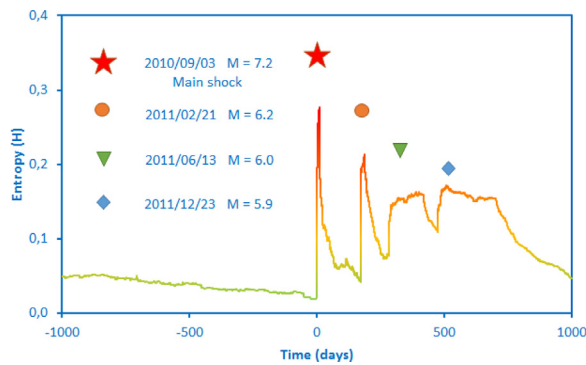


Fig. 6. Entropy, H , versus time (in days with respect to the date of the main event; that is, 4 September 2010) during the Christchurch sequence. The windowing process was carried out with a moving window width starting at $W = 1500$ earthquakes. Despite different windowing process, the results are qualitatively identical to those in Fig. 5.

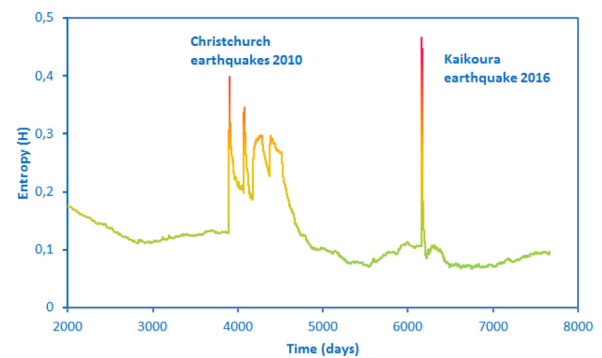


Fig. 8. Entropy, H , versus time (in days with respect to 1 January 2000) for the NZ2 catalogue (Christchurch and Kaikoura seismic sequences). The windowing process was carried out with a moving window (to avoid memory effects) width starting at $W = 1500$ earthquakes (for which relative errors are $< 1\%$). The two sequences can be recognised by abrupt variations in H .

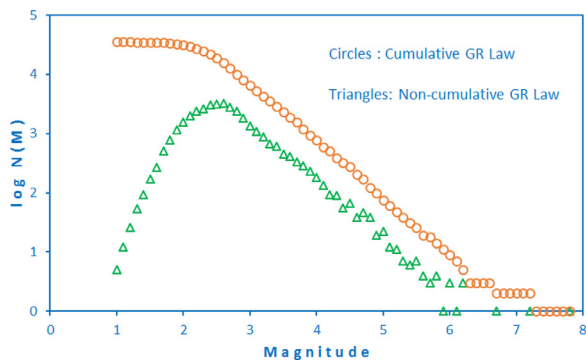


Fig. 7. Gutenberg-Richter (GR) law for the Christchurch and Kaikoura seismic sequences. Orange circles indicate the cumulative number of earthquakes; green triangles denote the non-cumulative number of earthquakes. Based on the Maximum Curvature (MAXC) technique [18], we selected a magnitude threshold of $M_0 = 2.55$.

an independent event (e.g., Atzori et al. [64], Kaiser et al. [74]). Currently, there is no way to confirm the nature of the February earthquake [75]; which could have been and aftershock or a subsequent event in another part of the seismic system that would not have occurred without the first (i.e., not an aftershock but a triggered

earthquake). For the Kaikoura earthquake, the unprecedented complexity of the rupture process [65], with multiple blocks of crust breaking simultaneously along more than a 100 km, does not fit with standard earthquake generation models. These factors highlight the usefulness of techniques such as the one presented here in terms of monitoring seismic activity.

However, although the methodology used here may be useful in the field of seismic prediction, two important issues must be considered. First, changes in H are detected both before and after the main earthquake. Further studies are necessary to determine, without prior knowledge of how a series will continue, how H values will evolve in the immediate future. In other words, an absolute scale of entropy is necessary. This has recently been achieved [76] using fluctuations of entropy change under the time reversal of entropy over natural time [77]. This considers the sequential order of events, and thus captures the dynamic entropy characteristics of the system, which differs essentially from statistical entropy (Shannon entropy).

The second consideration falls within the spatial domain. This work always takes into consideration a spatially limited seismic system. However, the expansion of the technique over a larger area (e.g., the entire Pacific plate border) presents difficulties, since it is necessary to connect the variation in H to a point. That is, it is not

enough to simply detect an increase in H ; one must also determine where the increase is located. The authors of this work are currently working on a 'microzone' of regions within the southern Iberian Peninsula that could allow for spatial, and not just temporal, monitoring of H .

5. Conclusions

In this study, we proposed the use of the Second Law of Thermodynamics (i.e., entropy, H) as an indicator of the equilibrium state of seismically active regions. This hypothesis was tested using two earthquake sequences on the South Island of New Zealand. Moreover, we compiled a detailed review of entropy (Appendix A). It is common in the scientific literature to speak about the evolution of entropy towards maximum values following the Second Law of Thermodynamics; however, it has been emphasised that entropy is a function of state and, as such, does not depend on time. However, it is the Boltzmann H function, identified with entropy and usually known as such, which is used to study the evolution of any system, and especially complex systems such as the Earth's crust and the earthquakes occurring within it. One of the main objectives of our review was to show the exportability of some classical concepts of Thermodynamics to others scientific fields, including the study of non-linear phenomena such as earthquakes.

Secondly, we developed a new methodology to identify the occurrence of an earthquake with an irreversible transition within a seismic system. This methodology is systematic, and its goal is to calculate the H function for a seismic system in which earthquakes are occurring (i.e., that is in a metastable state). Furthermore, we have presented an innovative approach for evaluating the error in entropy (H) values, which allows us to better interpret our results.

Our results, based on analysis of the 2010 M 7.2 Christchurch seismic crisis, show that sudden changes in entropy are associated with the occurrence of earthquakes. Moreover, it is possible to detect earthquakes considered as aftershocks or those that are subsequent to a previous event in another part of the seismic system but that would not have occurred without the first (i.e., not an aftershock but a triggered earthquake).

Finally, based on analysis of both the 2010 M 7.2 Christchurch and 2016 M 7.8 Kaikoura seismic sequences, we found that entropy changes associated with the occurrence of a subsequent large earthquake, separated in time from the first and with H having returned to the original values, again increase considerably.

Data availability

The seismic catalogue was obtained from GeoNet, a collaboration between GNS Science and the Earthquake Commission of New Zealand (<https://www.geonet.org.nz>). The data that support the findings of this study are available from the corresponding author upon reasonable request.

Declaration of Competing Interest

The authors declare that they have no known competing financial interests or personal relationships that could have appeared to influence the work reported in this paper.

CRedit authorship contribution statement

A. Posadas: Conceptualization, Methodology, Software, Supervision. **J. Morales:** Data curation, Writing – original draft. **J.M. Ibañez:** Writing – original draft, Visualization. **A. Posadas-Garzon:** Formal analysis, Writing – review & editing.

Acknowledgments

We would like to express our gratitude to GeoNet for making available the data used in this work. This work was partially supported by the RNM104 and RNM194 (Research Groups belonging to Junta de Andalucía, Spain), the Spanish National Projects [grant project PID2019-109608GB-I00], and the Junta de Andalucía Project [grant project A-RNM-421-UGR18]. English language editing was performed by Tornillo Scientific.

Supplementary materials

Supplementary material associated with this article can be found, in the online version, at [doi:10.1016/j.chaos.2021.111243](https://doi.org/10.1016/j.chaos.2021.111243).

Appendix A [1–117]

The concept of entropy and its connection to the Second Law of Thermodynamics was proposed by Clausius in 1865 [78]: "An uncompensated transmission of heat from a colder body to a warmer body can never occur". From this principle, Clausius discovered that entropy (S) is a state function that can be used to present the Second Law:

$$\Delta S \geq \Delta Q/T \quad (A1)$$

where ΔQ is the heat added to the system and T is the system's temperature. A few years later, Boltzmann realised that entropy could be used to connect the microscopic motion of particles to the macroscopic world; in his analysis, entropy is proportional to the number of accessible micro-states of the system (Ω) and is expressed by the famous Boltzmann equation:

$$S = k \ln \Omega \quad (A2)$$

where k is Boltzmann's constant. Ben-Naim [79] stated that, at first glance, Boltzmann's entropy and Clausius' entropy are absolutely different; however, there is complete agreement calculating changes of entropy using the two methods. Moreover, Boltzmann defined a function $H(t)$ [80]:

$$H(t) = \int^f (R, p, t) \log f(R, p, t) dR dp \quad (A3)$$

based on the position (R) and momenta (p) distribution $f(R, p, t)$ for a given time t and proved, now known as Boltzmann's H -theorem, that:

$$\frac{dH(t)}{dt} \leq 0 \quad (A4)$$

and at equilibrium:

$$\frac{dH(t)}{dt} = 0, \quad t \rightarrow \infty \quad (A5)$$

From this theorem, function $-H(t)$ always increases with time, and at equilibrium it reaches a maximum. Ben-Naim [79] showed that we can obtain entropy from the following equivalent formulas (up to a multiplicative constant):

$$S = \max_{\text{over all } t's} [-H(t)] \quad (A6)$$

and:

$$S = \lim_{t \rightarrow \infty} [-H(t)] \quad (A7)$$

After this theorem, although entropy is a state function and, as such, it is not function of time, time has often been identified as a behaviour of entropy and is included in the $-H(t)$ function of Boltzmann. Thus, when we state that the entropy of the universe always increases, we mean that the $-H(t)$ function always increases.

The generalization of Boltzmann's entropy for systems described by other macroscopic variables reflects Gibbs [81] and can be written as:

$$S = -k \sum_{i=1}^{\Omega} p_i \log p_i \tag{A8}$$

where p_i is the probability of the system being in the i -th state. If we have infinite possible states, then:

$$S = -k \int^p (\xi) \ln p(\xi) d\xi \tag{A9}$$

Shannon [82] and Shannon and Weaver [83] introduced Boltzmann-Gibbs's entropy concept into communication theory and defined the measure of information as:

$$I(p) = \sum_{i=1}^W p_i \log p_i \tag{A10}$$

where p is the distribution of states, p_i is the relative frequency for each event i , and W is the number of possible states. The function $I(p)$ is called 'Shannon information' because it is a measure of knowledge; therefore, Majewski [84] highlighted that $-I(p)$ denotes a lack of knowledge or ignorance. Clearly, $I(p)$ is always negative or zero; as such, it is possible to define the 'Shannon entropy' or 'Shannon information entropy' as the negative information measure; that is:

$$S(p) = -I(p) = - \sum_{i=1}^W p_i \log p_i \tag{A11}$$

which is always positive or zero. Probably, it would be better to note Shannon entropy with the symbol H since it is a measure of information [85] or the lack of information.

Some (relatively) recent research carried out in the field of information theory suggests that the above expressions can be generalised. Thus, Tsallis [86] proposed the use of:

$$S_{\tau} = \frac{k}{\tau - 1} \left(1 - \sum_{i=1}^W p_i^{\tau} \right) \tag{A12}$$

where τ is a real number called the entropic index. The standard distribution that characterises Boltzmann-Gibbs statistics is a particular case of Tsallis entropy in the limit of $\tau = 1$.

Regardless of the entropy used, the classical formulation of the Second Law of Thermodynamics establishes that:

$$\frac{dS}{dt} \geq 0 \tag{A13}$$

where dS can be split in two parts. First, the variation of the entropy produced inside the system (dS_i), and second, the transfer of entropy outside the system (dS_o). Then:

$$dS_i + dS_o \geq 0 \tag{A14}$$

If the system is an isolated one, then $dS_o = 0$ and it is possible to conclude that:

$$dS_i \geq 0 \tag{A15}$$

Majewski and Teisseyre [87] noted that the equal sign applies to the state of equilibrium, whereas the unequal sign applies to entropy production due to irreversible processes occurring inside the system (for example, irreversible strains such as those resulting from faulting processes in the crust). Thus, only in irreversible processes does the production of entropy occur and, therefore, the Second Law of Thermodynamics expresses that if any irreversible process advance in time, there is always an entropy increase.

Appendix B

The Second Law of Thermodynamics has been widely used in seismology as an indicator of the evolution of a system (e.g., Rundle et al. [88], Sornette and Werner [89]). In addition, several authors have found that entropy is the most convenient tool for characterising a statistical process (e.g., Apostol and Cune [16], who explain the Vancrea earthquakes); moreover, it is a reliable parameter to characterise the critical point where an earthquake happens (e.g., De Santis et al. [15] in Italian case studies of the L'Aquila and Colfiorito earthquakes).

In geophysics in general, but in seismology, in particular, the Second Law and entropy were introduced from statistical physics to measure the disorder produced by seismic activity. A number of studies have shown that complexity in earthquake processes can be characterised by entropy [90]. Most try to elucidate if there is a correlation between changes in entropy values and the occurrence of an earthquake.

Telesca et al. [91] found anomalous behaviour of Shannon entropy H in a 1983–2003 catalogue of seismicity in Central Italy; the anomaly is associated with stronger earthquakes. Main and Naylor [92] derived an analytical expression for entropy production and tested if the Second Law is a thermodynamic driver for a self-organised criticality state, in which elastic strain is near-critical and the rupture of materials could be reached (i.e., earthquake generation). Meanwhile, Machado and Lopes [93] and Lopes and Machado [94] used the Second Law to characterise the statistical distribution of earthquakes throughout the world, from 1963 to 2012, and concluded that entropy could represent the interrelation between the studied data. Specifically, they made use of the Kullback-Leibler formula [95] based on Shannon entropy.

A remarkable application was revealed by Akopian [96] in a study of the devastating 2011 M 9.1 Tohoku (Japan) earthquake [97]; in that work, the author used entropy to mathematically model the preparatory process that led to the earthquake. The same earthquake was studied by Sarlis et al. [98] by means of natural time analysis, a useful technique for analysing seismicity [99], and physiological time series [100]; they showed that the entropy of seismicity in natural time under time reversal changed sharply 2 months before the earthquake. Varotsos et al. [101] applied natural time analysis to study the Tsallis entropy q index [102] before the earthquake, and found that the index grew before this mega-event.

Shannon entropy and the fractal dimension was used by Bresnan et al. [103] to study seismic sequences before and after earthquakes in Italy and Slovenia. Regional Entropy of Seismic Information (RESI) was proposed by Ohsawa [104] to detect short-term precursors to the activation of earthquakes; clusters of earthquakes were introduced as microstates when computing entropy.

The concept of nowcasting was defined by Rundle et al. [105]; nowcasting is a method in which proxy data are used to estimate the current dynamic state of a driven complex system (such as an earthquake). Rundle et al. [105] incorporated measures of Shannon information entropy. Also, more recently, Akopian [106] explained the double earthquake phenomenon (earthquakes close in time, place, and magnitude) using the seismic entropy method; they attempted to clarify the nature of occurrence for earthquake forecasting and classified some of the features in seismic systems located in different seismotectonic situations, such as the Altai (Kuril Islands), central United States, and Pakistan.

In parallel, a series of notable works [107] introduced seismic noise entropy to detect preparation processes for strong earthquakes; the authors suggested that changes in the temporal and spatial structure of seismic noise in Japan and California are precursors to large earthquakes. The properties of seismic noise entropy from continuous records of the global network of broadband seismic stations from 1997 to 2019 were analysed.

Shannon entropy is not only used to examine the occurrence of earthquakes. For instance, the interevent-time and interevent-distance series of seismic events in Egypt, from 2004 to 2010, were studied by Telesca et al. [108] using Shannon entropy and the Fisher Information Measure. Vogel et al. [109] successfully proposed a method based on information theory to detect phase transitions in magnetism and applied it to Chilean earthquakes. [110]. Telesca et al. [111] combined measures of magnitude (Shannon entropy and Fisher information) to distinguish between tsunamigenic and non-tsunamigenic earthquakes in a sample of major earthquakes. The same method was used by Telesca et al. [112] to confirm the correlation between the properties of geoelectrical signals and crustal deformation at three sites in Taiwan. The spatial heterogeneity (and complexity of spatial point patterns) for a catalogue of earthquake events in Chile was analysed by Nicolis et al. [113] by adopting a combined Shannon entropy and wavelet-based approach. Vargas et al. [114] improved the performance of a genetic algorithm to optimise the test mathematical functions by determining the initial populations with the entropy of Shannon. Recently, Metin-Karakaş and Çalik [115] employed entropy approximations (Tsallis, Shannon, and Rényi entropy) to introduce the volatile concept for the Anatolian fault line during the period 1990 to 2019. Even in social science fields associated with earthquakes, Shannon entropy has been used to study the emergency rescue coordination relationship [116] and to evaluate social vulnerability [117].

References

- Ben-Naim A. "Discover entropy and the second law of thermodynamics. Singapore: World Scientific; 2010.
- Ben-Naim A. *Entropy the truth the whole truth and nothing but the truth*. Singapore: World Scientific; 2016.
- Schoenmaker J. Historical and physical account on entropy and perspectives on the second law of thermodynamics for astrophysical and cosmological systems. *Entropy* 2014;16:4420–42. doi:10.3390/e16084420.
- Ostad-Ali-Askari K, Su R, Liu L. Water resources and climate change. *J Water Clim Change* 2018;9(2):239. doi:10.2166/wcc.2018.999.
- Kato S, Rose FG. Global and regional entropy production by radiation estimated from satellite observations. *J Clim* 2020;33(8):2985–3000. doi:10.1175/JCLI-D-19-0596.1.
- Phillips SJ, Anderson RP, Schapire RE. Maximum entropy modeling of species geographic distributions. *Ecol Model* 2006;190(3–4):231–59. doi:10.1016/j.ecolmodel.2005.03.026.
- Ostad-Ali-Askari K, Shayannejad M. Quantity and quality modelling of groundwater to manage water resources in Isfahan-Borkhar Aquifer. *Environ Develop Sustain* 2021;23(3). doi:10.1007/s10668-021-01323-1.
- Deltete RJ. *Entropy in chemistry*. In: Woody AI, Hendry RF, Needham P, editors. *Philosophy of chemistry volume 6 of the philosophy of science*. North-Holland; 2012. p. 495–506. <https://doi.org/10.1016/B978-0-444-51675-6.50031-1>.
- Osanova BK. Calculating Information Entropy of Language Texts. *World Appl Sci J* 2013;22(1):41–5. doi:10.5829/jidosi.wasj.2013.22.01.2964.
- Mavrofidis T, Kameas A, Papageorgiou D, Los A. On the entropy of social systems: a revision of the concepts of entropy and energy in the social context. *Syst. Res. Behav. Sci.* 2011;28(4):353–68. doi:10.1002/sres.1084.
- Akopian ST. Open dissipative seismic systems and ensembles of strong earthquakes: energy balance and entropy funnels. *Geophys J Int* 2015;201:1618–41. doi:10.1093/gji/ggv096.
- Pirnazari M, Hasheminasab H, Karimi AZ, Ostad-Ali-Askari K, Ghasemi Z, Haeri-Hamedani M, et al. The evaluation of the usage of the fuzzy algorithms in increasing the accuracy of the extracted land use maps. *Int J Glob Environ Iss* 2018;17(4):307–21. doi:10.1504/IJGENVI.2018.095063.
- De Santis A, Cianchini G, Qamili E, Frepoli A. The 2009 L'Aquila (central Italy) seismic sequence as a chaotic process. *Tectonophysics* 2010;496:44–52. doi:10.1016/j.tecto.2010.10.005.
- Akopian ST, Kocharian AN. Critical behaviour of seismic systems and dynamics in ensemble of strong earthquakes. *Geophys J Int* 2014;196:580–99.
- De Santis A, Abbattista C, Alfonsi L, Amoroso L, Campuzano S, Carbone M, Cesaroni C, Cianchini G, De Franceschi G, De Santis A, Di Giovambattista R, Marchetti D, Martino L, Perrone L, Piscini A, Rainone M, Soldani M, Spogli L, Santoro F. Geosystemics view of earthquakes. *Entropy* 2019;21:412–42.
- Apostol BF, Cune LC. Entropy of earthquakes: application to Vrancea earthquakes. *Acta Geophys* 2021. doi:10.1007/s11600-021-00550-4.
- De Santis A, Cianchini G, Favali P, Beranzoli L, Boschi E. The Gutenberg-Richter law and entropy of earthquakes: two case studies in central Italy. *Bull Seism Soc Am* 2011;101:1386–95.
- Wiemer S, Wyss M. Minimum magnitude of complete reporting in earthquake catalogs: examples from Alaska, the Western United States, and Japan. *Bull Seismol Soc Am* 2000;90:859–69. doi:10.1785/0119990114.
- Gutenberg B, Richter CF. Frequency of earthquakes in California. *Bull Seismol Soc Am* 1944;34:185–8.
- Jimenez A, Tiampo KF, Levin S, Posadas A. Testing the persistence in earthquake catalogs: the Iberian Peninsula. *Europhys Lett* 2006;73:171–7. doi:10.1209/epl/i2005-10383-8.
- Frohlich C, Davis SD. Teleseismic b values; Or, much ado about 1.0. *J Geophys Res* 1993;98:631–44. doi:10.1029/92JB01891.
- Wesnouslyk SG. Crustal deformation processes and the stability of the Gutenberg-Richter relationship. *Bull Seismol Soc Am* 1999;89(4):1131–7.
- Singh C, Singh A, Chadha RK. Fractal and b-value in Eastern Himalaya and Southern Tibet. *Bull Seismol Soc Am* 2009;99(6):3529–33. doi:10.1785/0120090041.
- Turcotte R. *Fractals and chaos in geology and geophysics*. Cambridge Cambridge: University Press; 1997.
- Wiemer S, McNutt S. Variations in the frequency-magnitude distribution with depth in two volcanic areas: Mount St. Helens, Washington, and Mt. Spurr, Alaska. *Geophys Res Lett* 1997;24(2):189–92. doi:10.1029/96GL03779.
- Mogi K. Regional variation in magnitude-frequency relation of earthquake. *Bull Earthq Res Inst* 1967;45:313–25.
- Scholz CH. The frequency-magnitude relation of micro-fracturing in rock and its relation to earthquakes. *Bull Seismol Soc Am* 1968;58:399–415.
- von Ketelhodt J, Ligaraba D, Durrheim RJ. Analysis of the Gutenberg-Richter b-values of overlapping seismic clusters with application to Cooke 4 gold mine. In: Joughin W, editor. *Proceedings of the Ninth International Conference on Deep and High Stress Mining. The Southern African Institute of Mining and Metallurgy*; 2019. p. 335–46. doi:10.36487/ACG_rep/1952_25_Durrheim.
- Wiemer S, Benoit J. Mapping the b-value anomaly at 100 km depth in the Alaska and New Zealand subduction zones. *Geophys Res Lett* 1996;23:1557–60. doi:10.1029/96GL01233.
- Wiemer S, McNutt SR, Wyss M. Temporal and three-dimensional spatial analyses of the frequency-magnitude distribution near Long Valley Caldera, California. *Geophys J Int* 1998;134:409–21. doi:10.1046/j.1365-246x.1998.00561.x.
- Gibowicz SJ, Lasocki S. Seismicity induced by mining: ten years later. *Adv Geophys* 2001;44:39–181. doi:10.1016/S0065-2687(00)80007-2.
- Monterroso D, Kulhanek O. Spatial variations of b-values in the subduction zone of Central America. *Geofisica Inter* 2003;42:1–13.
- Monterroso D. Seismic precursory potential of temporal variation of b-value: five case studies in Central America. *Comprehensive Summaries of Uppsala Dissertations from the Faculty of Sci Technol* 2003;897:17.
- Nuannin P, Kulhanek O, Persson L, Tillman K. Forecasting of increasing induced seismicity in the Zinkgruvan mine, Sweden, by using temporal variations of b-values. *Acta Montana A* 2002;21:13–25.
- Berrill JB, Davis RO. Maximum entropy and the magnitude distribution. *Bull Seismol Soc Am* 1980;70:1823–31.
- Shen PY, Mansinha L. On the principle of maximum entropy and the earthquake frequency-magnitude relation. *Geophys J R Astr Soc* 1983;74:777–85. doi:10.1111/j.1365-246X.1983.tb01903.x.
- Main I, Burton PW. Information theory and the earthquake frequency-magnitude distribution. *Bull Seismol Soc Am* 1984;74:1409–26.
- Feng L, Luo G. The relationship between seismic frequency and magnitude as based on the Maximum Entropy Principle. *Soft Comput* 2009;13:979–83. doi:10.1007/s00500-008-0340-x.
- Aki K. Maximum likelihood estimate of b in the formula $\log(N) = a - bm$ and its confidence limits. *Bull Earthq Res Inst Tokyo Univ* 1965;43:237–9.
- Utsu T. A method for determining the value of b in a formula $\log n = a - bm$ showing the magnitude-frequency relation for earthquakes. *Geophys Bull Hokkaido Univ* 1965;13:99–103.
- Marzocchi W, Sandri L. A review and new insights on the estimation of the b-value and its uncertainty. *Ann Geophys* 2003;46(6):1271–82. doi:10.4401/ag-3472.
- Lolli B, Gasperini P. Aftershock hazard in Italy Part I: estimation of time-magnitude distribution model parameters and computation of probabilities of occurrence. *J Seismol* 2003;7:235–57. doi:10.1023/A:1023588007122.
- Utsu T. A statistical significance test of the difference in b-value between two earthquake groups. *J Phys Earth* 1966;14:34–40. doi:10.4294/jpe.1952.14.37.
- Bender B. Maximum likelihood estimation of b-values for magnitude grouped data. *Bull Seismol Soc Am* 1983;73(3):831–51.
- Shi Y, Bolt BA. The standard error of the magnitude-frequency b value. *Bull Seism Soc Am* 1982;72:1677–87.
- Amorèse D, Grasso JR, Rydelek PA. On varying b-values with depth: results from computer-intensive tests for Southern California. *Geophys J Int* 2010;180(1):347–60. doi:10.1111/j.1365-246X.2009.04414.x.
- Mignan A, Woessner J. Estimating the magnitude of completeness for earthquake catalogs. *Community Online Resource for Statistical Seismicity Analysis*; 2012. doi:105078/corssa-00180805.
- Rydelek PA, Sacks IS. Testing the completeness of earthquake catalogs and the hypothesis of self-similarity. *Nature* 1989;337:251–3. doi:10.1038/337251a0.
- Woessner J, Wiemer S. Assessing the quality of earthquake catalogues: estimating the magnitude of completeness and its uncertainty. *Bull Seismol Soc Am* 2005;95:684–98. doi:10.1785/0120040007.
- Amorèse D. Applying a change-point detection method on frequency-magnitude distributions. *Bull Seismol Soc Am* 2007;97:1742–9. doi:10.1785/0120060181.

- [51] Kvaerna T, Ringdal F. Seismic threshold monitoring for continuous assessment of global detection capability. *Bull Seismol Soc Am* 1999;89:946–59.
- [52] Schorlemmer D, Woessner J. Probability of detecting an earthquake. *Bull Seismol Soc Am* 2008;98:2103–17. doi:10.1785/0120070105.
- [53] D'Alessandro A, Luzio D, D'Anna G, Mangano G. Seismic network evaluation through simulation: an application to the Italian national seismic network. *Bull Seismol Soc Am* 2011;101:1213–32. doi:10.1785/0120100066.
- [54] Zúñiga F, Wyss M. Inadvertent changes in magnitude reported in earthquake catalogs: their evaluation through b-value estimates. *Bull Seismol Soc Am* 1995;85:1858–66.
- [55] Ogata Y, Katsura K. Analysis of temporal and spatial heterogeneity of magnitude frequency distribution inferred from earthquake catalogues. *Geophys J Int* 1993;3(113):727–38. doi:10.1111/j.1365-246X.1993.tb04663.x.
- [56] Cao AM, Gao SS. Temporal variations of seismic b-values beneath north-eastern Japan island arc. *Geophys Res Lett* 2002;29(9):1334. doi:10.1029/2001GL013775.
- [57] Utsu T. Representation and analysis of the earthquake size distribution: a historical review and some new approaches. *Pure Appl Geophys* 1999;155:509–35. doi:10.1007/s000240050276.
- [58] DeMets C, Gordon RG, Argus DF, Stein S. Effect of recent revisions to the geomagnetic time scale on estimates of current plate motions. *Geophys Res Lett* 1994;21:2191–4. doi:10.1029/94GL02118.
- [59] Beavan J, Wallace LM, Palmer N, Denys P, Ellis S, Fournier N, et al. New Zealand GPS velocity field: 1995–2013. *N Z J Geol Geophys* 2016;59(1):5–14. doi:10.1080/00288306.2015.1112817.
- [60] Grapes R, Downes G. The 1855 Wairarapa, New Zealand, earthquake. *Bull N Z Soc Earthq Eng* 1997;30(4):271–368. <https://doi.org/10.5459/bnzsee.30.4.271-368>.
- [61] Campbell JK, Pettinga JR, Jørgens R. The tectonic and structural setting of the 4 September 2010 Darfield (Canterbury) earthquake sequence, New Zealand. *N Z J Geol Geophys* 2012;55:155–68. <https://doi.org/10.1080>.
- [62] Yang W, O'Donnell A. Earthquake risk in New Zealand: a major model update. *AIR currents* article 2019. <https://www.air-worldwide.com/publications/air-currents/2019/Earthquake-Risk-in-New-Zealand-A-Major-Model-Update/>.
- [63] Potter SH, Becker JS, Johnston DM, Rossiter KP. An overview of the impacts of the 2010–2011 Canterbury earthquakes. *Int J Disaster Risk Reduct* 2015;4(1):6–14. doi:10.1016/j.ijdrr.2015.01.014.
- [64] Atzori S, Tolomei C, Antonioli A, Meryman Boncori JP, Bannister S, Trasatti E, et al. The 2010–2011 Canterbury, New Zealand, seismic sequence: multi-pole source analysis from InSAR data and modelling. *J Geophys Res* 2012;117:B08305. doi:10.1029/2012JB009178.
- [65] Hollingsworth J, Ye L, Avouac JP. Dynamically triggered slip on a splay fault in the Mw 7.8, 2016 Kaikoura (New Zealand) earthquake. *Geophys Res Lett* 2017;44:3517–25. doi:10.1002/2016GL072228.
- [66] Cesca S, Zhang Y, Mouslopoulou V, Wang R, Saul J, Savage M, et al. Complex rupture process of the Mw 7.8, 2016, Kaikoura earthquake, New Zealand, and its aftershock sequence. *Earth Planet Sci Lett* 2017;478:110–20. doi:10.1016/j.epsl.2017.08.024.
- [67] Parsons T, Ji C, Kirby E. Stress changes from the 2008 Wenchuan earthquake and increased hazard in the Sichuan basin. *Nature* 2008;454:509–10. doi:10.1038/nature07177.
- [68] Hainzl S, Zoller G, Kurths J, Zschau J. Seismic quiescence as an indicator for large earthquakes in a system of self-organized criticality. *Geophys Res Lett* 2000;27(5):597–600. doi:10.1029/1999GL011000.
- [69] Rudolf-Navarro A, Diosdado A, Angulo-Brown F. Seismic quiescence patterns as possible precursors of great earthquakes in Mexico. *Int J Phys Sci* 2010;5:651–70.
- [70] Ibañez JM, De Angelis S, Díaz-Moreno A, Hernández P, Alguacil G, Posadas A, et al. Insights into the 2011–2012 submarine eruption off the coast of El Hierro (Canary Islands, Spain) from statistical analyses of earthquake activity. *Geophys J Int* 2012;191(2):659–70. doi:10.1111/j.1365-246X.2012.05629.x.
- [71] Díaz-Moreno A, Ibañez JM, De Angelis S, García-Yegua A, Prudencio J, Morales J, et al. Seismic hydraulic fracture migration originated by successive deep magma pulses: the 2011–2013 seismic series associated to the volcanic activity of El Hierro Island. *J Geophys Res Solid Earth* 2015;120(11):7749–70. doi:10.1002/2015JB012249.
- [72] Langridge R, Dissen R, Rhoades D, Villamor P, Little T, Litchfield N, et al. Five thousand years of surface ruptures on the Wellington fault, New Zealand: implications for recurrence and fault segmentation. *Bull Seismol Soc Am* 2011;101:2088–107. doi:10.1785/0120100340.
- [73] Oth A, Kaiser AE. Stress release and source scaling of the 2010–2011 Canterbury, New Zealand earthquake. *Pure Appl Geophys* 2014;171:2767–82. doi:10.1007/s00024-013-0751-1.
- [74] Kaiser A, Holden C, Beavan J, Beetham D, Benites R, Celentano A, et al. The Mw 6.2 Christchurch earthquake of February 2011: Preliminary report. *N Z J Geol Geophys* 2012;55(1):67–90. doi:10.1080/00288306.2011.641182.
- [75] Stramondo S, Kyriakopoulos C, Bignami C, Chini M, Melini D, Moro M, et al. Did the September 2010 (Darfield) earthquake trigger the February 2011 (Christchurch) event? *Sci Rep* 2011;1:98. doi:10.1038/srep00098.
- [76] Varotsos PA, Skordas ES, Sarlis NV. Fluctuations of the entropy change under time reversal: further investigations on identifying the occurrence time of an impending major earthquake. *Europhys Lett* 2020;130:29001. doi:10.1209/0295-5075/130/29001.
- [77] Varotsos PA, Sarlis NV, Skordas ES, Tanaka H. A plausible explanation of the b-value in the Gutenberg-Richter law from first Principles. *Proc Jpn Acad B* 2004;80(9):429–34. doi:10.2183/pjab.80.429.
- [78] Clausius R. *Mechanical theory of heat*. London, UK: John van Voorst; 1865.
- [79] Ben-Naim A. Entropy and time. *Entropy* 2020;22:430. doi:10.3390/e22040430.
- [80] Brush SG. *Statistical physics and the atomic theory of matter, from Boyle and Newton to Landau and Onsager*. Princeton: Princeton University Press; 1983.
- [81] Zupanovic P, Domagoj K. Relation between Boltzmann and Gibbs entropy and example with multinomial distribution. *J. Phys. Commun.* 2018;2:045002. doi:10.1088/2399-6528/aab7e1.
- [82] Shannon CE. A mathematical theory of communication. *Bell Syst Tech J* 1948.
- [83] Shannon CE, Weaver W. *The mathematical theory of communication*. The Board of Trustees of the University of Illinois; 1949.
- [84] Majewski E. Thermodynamics of chaos and fractals applied: evolution of the earth and phase transformations. In: Teisseyre R, Majewski E, editors. *Earthquake thermodynamics and phase transformations in the Earth's interior*. Academic Press; 2001. p. 25–78.
- [85] Ben-Naim A. Entropy, Shannon's measure of information and Boltzmann's H-theorem. *Entropy* 2017;19:48. doi:10.3390/e19020048.
- [86] Tsallis C. Possible generalization of Boltzmann-Gibbs statistics. *J Stat Phys* 1988;52:479. <https://doi.org/10.1007/BF01016429>.
- [87] Majewski E, Teisseyre R. Earthquake thermodynamics. *Tectonophysics* 1997;277:219–33. doi:10.1016/S0040-1951(97)00088-7.
- [88] Rundle JB, Turcotte DL, Shcherbakov R, Klein W, Sammis C. Statistical physics approach to understanding the multiscale dynamics of earthquake fault systems. *Rev Geophys* 2003;41:1019–49.
- [89] Sornette D, Werner MJ. Statistical physics approaches to seismicity. In: Meyers RA, editor. *Encyclopedia of complexity and systems science*. Springer; 2009. p. 7872–91.
- [90] Vogel E, Brevis F, Pastén D, Muñoz V, Miranda R, Chian A. Measuring the seismic risk along the Nazca-Southamerican subduction front: Shannon entropy and mutability. *Nat Hazards Earth Syst Sci* 2020;20:2943–60. doi:10.5194/nhess-20-2943-2020.
- [91] Telesca L, Lapenna V, Lovallo M. Information entropy analysis of Umbria-Marche region (central Italy). *Nat Hazards Earth Syst Sci* 2004;4:691–5. doi:10.5194/nhess-4-691-2004.
- [92] Main G, Naylor M. Entropy production and self-organized (sub)criticality in earthquake dynamics. *Phil Trans R Soc A* 2010;368:131–44. doi:10.1098/rsta.2009.0206.
- [93] Machado JAT, Lopes AM. Analysis and visualization of seismic data using mutual information. *Entropy* 2013;15:3892–909. doi:10.3390/e15093892.
- [94] Lopes AM, Machado JAT. Integer and fractional-order entropy analysis of earthquake data series. *Nonlinear Dyn* 2016;84:79–90. doi:10.1007/s11071-015-2231-x.
- [95] Posadas A, Hirata T, Vidal F. Information theory to characterize spatiotemporal patterns of seismicity in the Kanto Region. *Bull Seism Soc Am* 2002;92(2):600–10. doi:10.1785/0120000247.
- [96] Ts Akopian AS. Seismic systems of Japan: entropy and monitoring of the Tohoku earthquake. *March 11, 2011. Seis Instr* 2014;50(4):347–68. doi:10.3103/S0747923914040021.
- [97] Ammon CJ, Lay T, Kanamori H, Cleveland M. A rupture model of the 2011 off the Pacific coast of Tohoku Earthquake. *Earth Planet Space* 2011;63:693–6. doi:10.5047/eps.2011.05.015.
- [98] Sarlis NV, Skordas ES, Varotsos PA. A remarkable change of the entropy of seismicity in natural time under time reversal before the super-giant M9 Tohoku earthquake on 11 March 2011. *Europhys Lett* 2018;124:29001–8. doi:10.1209/0295-5075/124/29001.
- [99] Varotsos PA, Sarlis NV, Skordas ES. Scale-specific order parameter fluctuations of seismicity in natural time before mainshocks. *Europhys Lett* 2011;96:59002. doi:10.1209/0295-5075/96/59002.
- [100] Varotsos PA, Sarlis NV, Skordas ES, Lazaridou MS. Identifying sudden cardiac death risk and specifying its occurrence time by analyzing electrocardiograms in natural time. *Appl Phys Lett* 2007;91:064106. doi:10.1063/1.2768928.
- [101] Varotsos PA, Sarlis NV, Skordas ES. Tsallis entropy index q and the complexity measure of seismicity in natural time under time reversal before the M9 Tohoku earthquake in 2011. *Entropy* 2018;20(10):757–73. doi:10.3390/e20100757.
- [102] Sotolongo O, Posadas A. Fragment-asperity interaction model for earthquakes. *Phys Rev Lett* 2004;92(4):048501. doi:10.1103/PhysRevLett.92.048501.
- [103] Bressan G, Barnaba C, Gentili S, Rossi G. Information entropy of earthquake populations in northeastern Italy and western Slovenia. *Phys Earth Planet Interiors* 2017;271:29–46. doi:10.1016/j.pepi.2017.08.001.
- [104] Ohsawa Y. Regional seismic information entropy to detect earthquake activation precursors. *Entropy* 2018;20:861. doi:10.3390/e20110861.
- [105] Rundle JB, Giguere A, Turcotte DL, Crutchfield JP, Donnellan A. Global seismic nowcasting with Shannon information entropy. *Earth Space Sci* 2019;6(1):191–7. doi:10.1029/2018EA000464.
- [106] Akopian ST. Double earthquakes, their nature, and forecast by the method of seismic entropy. *Seis Instr* 2019;55:196–208. doi:10.3103/S0747923919020026.
- [107] Lyubushin A. Global seismic noise entropy. *Front Earth Sci* 2020;8:558. doi:10.3389/feart.2020.611663.
- [108] Telesca L, Lovallo M, Mohamed AEEA, ElGabry M, El-hady S, Abou Eleenane KM, et al. Informational analysis of seismic sequences by applying the Fisher Information Measure and the Shannon entropy: an application to the 2004–2010 seismicity of Aswan area (Egypt). *Physica A* 2021;391:2889–97. doi:10.1016/j.physa.2011.12.047.

- [109] Vogel E, Saravia G, Cortez LV. Data compressor designed to improve recognition of magnetic phases. *Physica A* 2012;391:1591–601. doi:[10.1016/j.physa.2011.09.005](https://doi.org/10.1016/j.physa.2011.09.005).
- [110] Vogel EE, Saravia G, Pasten D, Munoz V. Time-series analysis of earthquake sequences by means of information recognizer. *Tectonophysics* 2017;712:723–8. doi:[10.1016/j.tecto.2017.06.031](https://doi.org/10.1016/j.tecto.2017.06.031).
- [111] Telesca L, Lovallo M, Chamoli A, Dimri VP, Srivastava K. Fisher-Shannon analysis of seismograms of tsunami genic and non-tsunamigenic earthquakes. *Physica A* 2013;392:3424–9. doi:[10.1016/j.physa.2013.03.049](https://doi.org/10.1016/j.physa.2013.03.049).
- [112] Telesca L, Lovallo M, Romano G, Konstantinou KI, Hsu HL, Chen CC. Using the informational Fisher-542 Shannon method to investigate the influence of long-term deformation processes on geoelectrical signals: an example from the Taiwan orogeny. *Physica A* 2014;414:340–51. doi:[10.1016/j.physa.2014.07.060](https://doi.org/10.1016/j.physa.2014.07.060).
- [113] Nicolis O, Mateu J. 2D Anisotropic wavelet entropy with an application to earthquakes in Chile. *Entropy* 2015;17:4155–72. doi:[10.3390/e17064155](https://doi.org/10.3390/e17064155).
- [114] Vargas M, Fuertes G, Alfaro M, Gatica G, Gutierrez S, Peralta M. The effect of entropy on the performance of modified genetic algorithm using earthquake and wind time series. *Complexity* 2018:4392036 2018. doi:[10.1155/2018/4392036](https://doi.org/10.1155/2018/4392036).
- [115] Metin-Karakaş A, Çalik S. Entropy method for earthquake volatility. *Sigma J Eng Nat Sci* 2020;38(1):329–48.
- [116] Rong H, Xuedong L, Guizhi Z, Yulin Y, Da W. An evaluation of coordination relationships during earthquake emergency rescue using entropy theory. *Cad. Saúde Pública, Rio de Janeiro* 2015;31(5):947–59. doi:[10.1590/0102-311X00039514](https://doi.org/10.1590/0102-311X00039514).
- [117] Jena R, Pradhan B. Earthquake social vulnerability assessment using entropy. *IOP Conf Ser Earth Environ Sci* 2020;540:012079. doi:[10.1088/1755-1315/540/1/012079](https://doi.org/10.1088/1755-1315/540/1/012079).